# A Novel Ultra-Wideband 80 GHz FMCW Radar System for Contactless Monitoring of Vital Signs

Siying Wang[1], Antje Pohl[2,3], Timo Jaeschke[4],
Michael Czaplik[5], Marcus Köny[2], Steffen Leonhardt[2], Nils Pohl[1]

*Abstract*— **In this paper an ultra-wideband 80 GHz FMCW-radar system for contactless monitoring of respiration and heart rate is investigated and compared to a standard monitoring system with ECG and $CO_2$ measurements as reference. The novel FMCW-radar enables the detection of the physiological displacement of the skin surface with submillimeter accuracy. This high accuracy is achieved with a large bandwidth of 10 GHz and the combination of intermediate frequency and phase evaluation. This concept is validated with a radar system simulation and experimental measurements are performed with different radar sensor positions and orientations.**

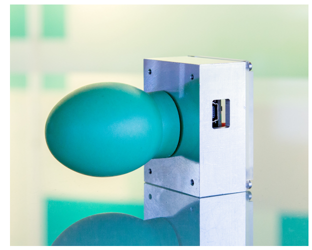

Fig. 1. FMCW-radar sensor with a teflon antenna.

## I. INTRODUCTION

Non contact detection of vital signs becomes increasingly important, especially for long-term home monitoring of patients with chronic diseases and for elderly people. Because of the aging society, the demand for healthcare at home applications rises continuously. Additionally, for neonates or patients with burn injuries, it is not feasible to place electrodes on the patients body for electrocardiographic monitoring, hence a contactless measurement method is required.

Radar systems were originally designed for detecting targets at large range and used primarily for air traffic control or sea navigation. In the early 1970s radar sensors were first considered for medical applications [1]. Nowadays, two radar techniques are mainly used for vital sign monitoring: The continuous wave (CW) Doppler radar [2-5] and the impulse ultra wide band (UWB) radar [6],[7]. The physiological movement of the body surface due to cardiac [8] and respiratory activity can be detected with both techniques from several meters distance [9]. The disadvantage of CW Doppler Radar is that other moving objects in front and behind the target will interfere with the CW radar signal, thus, it is difficult to distinguish the target from interfering objects. With the impulse UWB radar, a distance measurement is possible, but a high power needs to be send during the short period of the pulse.

Because of these drawbacks, a novel frequency modulated continuous wave (FMCW) radar sensor with 80 GHz center frequency and 10 GHz bandwidth is investigated, which results in distance measurement accuracy of micrometer (see Fig.1) [10],[11]. Furthermore the 80 GHz FMCW-radar enables a better spatial focusing compared to the commonly used UWB-radars, which operate only in the lower GHz range. With the FMCW-radar principle, a range profile can be determined using the intermediate frequency, hence target and disturbing objects can be separated spatially and filtered out. The FMCW-radar uses a frequency modulation with a continuous wave signal, therefore, the energy is not pulsed and a greater power efficiency can be achieved. The transmission power is 0.5 mW, which is about 10000 times lower than the official limit on radiation exposure [12].

## II. SYSTEM SIMULATION MODEL

In order to develop and verify algorithms for heart and respiration rate detection, a simulation model of the FMCW-radar system and the physiological movement was implemented.

### A. *FMCW-radar technique*

The FMCW-radar transmits a signal with periodic frequency modulation. The frequency decreases linearly during the chirp length $T_c$ (see Fig.2).

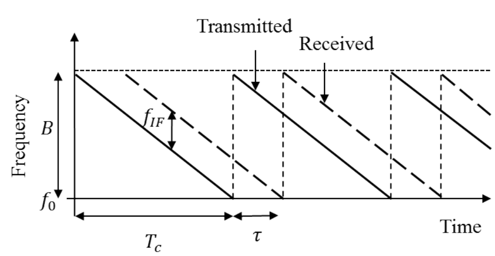


Fig. 2. FMCW downchirp of transmitted and received signal.

[1]Siying Wang and Nils Pohl are with Fraunhofer Institute for High Frequency Physics and Radar Techniques, 53343 Wachtberg, Germany

[2]Antje Pohl, Marcus Köny and Steffen Leonhardt are with Philips Chair of Medical Information Technology, RWTH Aachen University, 52074 Aachen, Germany

[3]Antje Pohl is with Department of Cardiovascular and Thoracic Surgery, University Hospital RWTH Aachen, 52074 Aachen, Germany

[4]Timo Jaeschke is with Institute for Integrated Systems, Ruhr-University Bochum, 44801 Bochum, Germany

[5]Michael Czaplik is with Department of Anaesthesiology, University Hospital RWTH Aachen, 52074 Aachen, Germany

The transmitted signal is reflected on the target and received with a time delay $\tau$, which is dependent on the distance $R$ between radar and target:

$$\tau = \frac{2R}{c_0}, \tag{1}$$

$c_0$ depicts the velocity of light. Because of the time delay, a frequency difference (also called intermediate frequency) $f_{\text{IF}}$ occurs between the transmitted and received signal:

$$f_{\text{IF}} = \frac{B}{T_c}\tau. \tag{2}$$

$B$ is the bandwidth of the signal and $T_c$ the chirp length. By detecting the frequency difference $f_{\text{IF}}$ the distance $R$ can be determined with

$$R = \frac{c_0}{2}\frac{T_c}{B} f_{\text{IF}}. \tag{3}$$

### B. Signal Model

The schematic diagram of the FMCW-radar principle is illustrated in Fig. 3. The transmitted downchirp signal $S_T(t)$

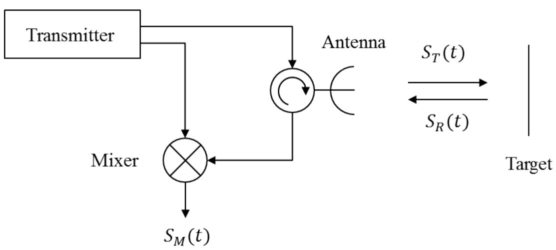


Fig. 3. Simulation of FMCW-radar system.

is modelled with following function:

$$S_T(t) = A_T \cdot cos(2\pi(f_0 + B)\cdot t - \pi\frac{B}{T_c}t^2). \tag{4}$$

$A_T$ is the signal amplitude and $f_0$ depicts the lowest frequency. The frequency decreases linearly and the phase $\phi$ changes quadratically with time:

$$\phi = 2\pi(f_0 + B)\cdot t - \pi\frac{B}{T_c}t^2. \tag{5}$$

The received signal $S_R(t)$ contains a time delay $\tau$ compared to the transmitted signal

$$S_R(t) = A_R \cdot cos(\phi(t - \tau)). \tag{6}$$

$A_R$ is the amplitude of the received signal. In the next step the transmitted and received signals are multiplied with a mixer and the low-pass filtered output signal can be modelled with

$$S_M(t) = A_M \cdot cos(-2\pi f_{\text{IF}}\cdot t + 2\pi(f_0 + B)\tau + \pi\frac{B}{T_c}\tau^2). \tag{7}$$

The mixed signal $S_M(t)$ contains the difference frequency $f_{IF}$, which can be detected to determine the distance $R$ between radar and target.
The displacement of the skin surface due to cardiac and respiratory activity is simulated with an overlap of two sinusoidal signals, one representing the heart and the other one the respiration signal. The simulated change in distance is illustrated in Fig. 4. The respiration signal is simulated with an amplitude of 4 mm and a frequency of 0.2 Hz (this corresponds to 12 breaths per minute). For the heart signal, an amplitude of 0.5 mm and a heart rate of 1.3 Hz was chosen (this corresponds to 72 beats per minute). In addition to the physiological movement, a constant distance of 1 m is added.

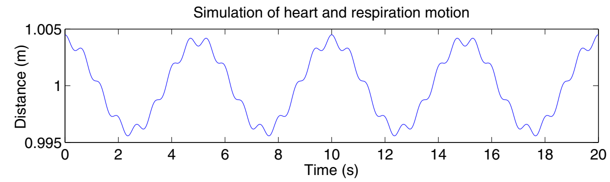


Fig. 4. Changing distance between the radar and the simulated heart and respiration movement.

### C. Algorithm for high-precision vital sign detection

The algorithm for the high accuracy detection of the vital signs is summarized in the flow chart of Fig. 5. The raw data received from the radar system is equivalent to the lowpass filtered output signal of the mixer. In the first step an FFT transformation with zero padding is calculated. With the background knowledge of the approximate distance to the test person, a region of interest can be selected in the frequency domain. All targets in front and behind the selected range can be omitted. The ability to filter out interfering objects in the range domain is a main advantage of the FMCW principle. Afterwards, a peak detection is performed to determine the difference frequency and hence the distance between radar and target. The peak detection process is optimized with an adaptive algorithm, which takes the previously detected peak positions into consideration to avoid large changes in distance which are caused by noise

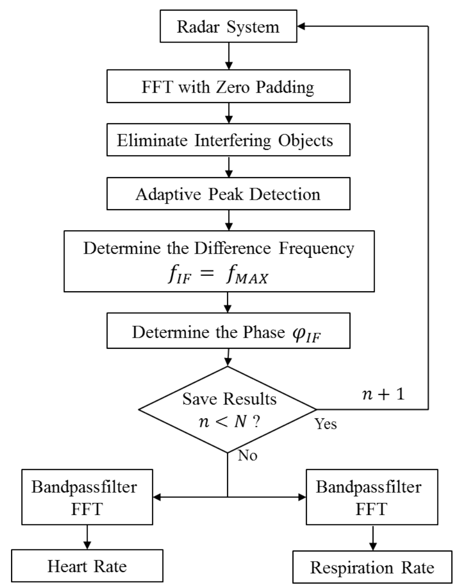


Fig. 5. Algorithm for detecting the vital signs in submillimeter range.

or movement artefacts. In the next step, the phase of the difference frequency is evaluated to enable the detection of the skin surface movement in submillimeter range. After calculating and saving all the distance values over time, bandpass filtering is applied to separate the heart from the respiration signal.

## III. Experimental Results

A set of measurements was performed (see Fig. 6) with the objective to validate and compare the radar measurements of the vital signs with a standard monitoring system. Therefore, the laboratory pilot study was initiated involving ten voluntary members of our working group.

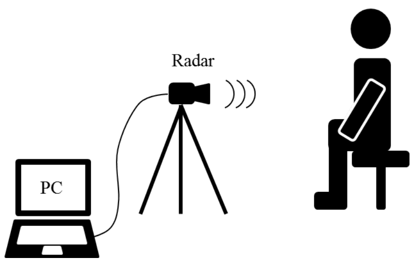


Fig. 6. Illustration of the measurement setup with probands sitting in front of the FMCW-radar system, which is connected to a PC.

The Philips MP70 monitor was used with the software SomnuCare to record the reference data [13]: The electrocardiogram (ECG) leads Einthoven I, II and III for heart rate monitoring and $CO_2$ changes equivalent to the respiratory rate.

TABLE I
Position and Orientation of the Radar

| Position | Orientation | Distance |
|---|---|---|
| 1 | Radar in front of the proband | 1 m |
| 2 | Radar at the back of the proband | 1 m |
| 3 | Radar at the left side of the proband | 1 m |
| 4 | Radar in front of the proband | 2 m |

The test persons were seated on a chair and the radar sensor was placed at four different positions, as listed in Table I. Measurements were performed from the front, back and left side of the test persons in 1 m distance and additionally from the front position in 2 m distance. In all positions the radar sensor was directed towards the thorax center and the vital signs were detected through clothing. The test persons were instructed to sit still during the measurement time of 100 s.

### A. Cross correlation of radar and reference signal

Fig. 7 illustrates one typical example of the measurement result for the respiration signal. It shows the $CO_2$ reference signal and the respiration signal detected with the phase evaluation of the radar sensor. The cross correlation of both signals is displayed at the bottom of Fig. 7, which is normalized so that the autocorrelation at zero lag equals 1. Because of the periodicity of the two compared signals, the cross correlation function has positive and negative maxima

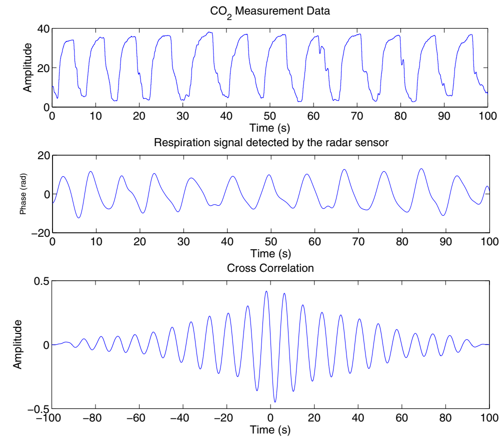


Fig. 7. Comparison of the reference $CO_2$ measurement and respiration signal measured with the radar sensor.

in nearly constant intervals. It can be clearly seen that both signals are correlated with a maximum correlation coefficient of 0.45. Fig. 8 illustrates one typical example of the heart signal measured with ECG and the radar sensor, as well as the cross correlation of both signals. The ECG and the heart

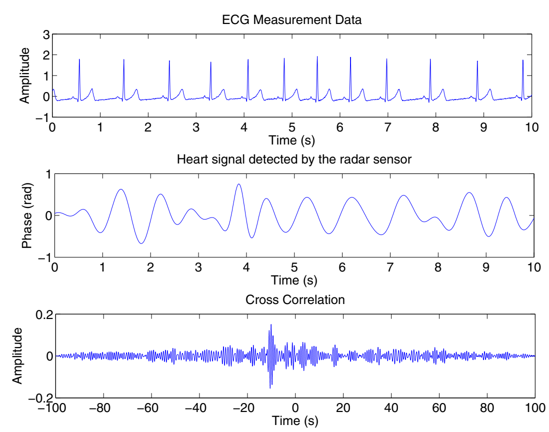


Fig. 8. Comparison of the reference ECG and heart signal measured with the radar sensor.

rate measured with the radar system show less correlation compared to the respiration signals. The movement of the skin surface due to cardiac activity is in the submillimeter range, hence it is more sensitive to noise and motion artifacts. However, the detection of a distinct peak at a time delay of -10.13 s, with a maximal correlation coefficient of 0.15 is possible. This indicates that the radar sensor did not only detect noise, but that the cardiac activity is contained in the radar sensor signal. Thus, these results demonstrate the feasibility of the detection of heart rate with the FMCW-radar system.

### B. Evaluation of various radar measurement positions

In the next step, the influence of different radar measurement positions (Table I) on the vital sign detection is investigated. These measurements were performed to analyse

TABLE II

RELATIVE ERROR IN (%) OF THE AVERAGE RESPIRATION RATE

| Position | Proband | | | | | | | | | | Median | Mean |
|---|---|---|---|---|---|---|---|---|---|---|---|---|
| | 1 | 2 | 3 | 4 | 5 | 6 | 7 | 8 | 9 | 10 | | |
| 1 | 0 | 4.03 | 18.45 | 9.09 | 6.45 | 5.51 | 0.69 | 7.33 | 26.27 | 11.4 | 6.89 | 8.92 ± 8.09 |
| 2 | 95.38 | 56.05 | 0 | 59.17 | 1.43 | 46.32 | 5.52 | 43.92 | 3.54 | 3.16 | 24.72 | 31.45 ± 33.3 |
| 3 | 1.49 | 28.57 | 23.16 | 5.22 | 9.52 | 25.79 | 13.39 | - | 9.49 | 6.85 | 9.52 | 13.72 ± 9.75 |
| 4 | 0 | - | 4.88 | 11.59 | 1.45 | 7.19 | 6.16 | 0 | - | 7.5 | 5.52 | 4.85 ± 4.11 |

TABLE III

RELATIVE ERROR IN (%) OF THE AVERAGE HEART RATE

| Position | Proband | | | | | | | | | | Median | Mean |
|---|---|---|---|---|---|---|---|---|---|---|---|---|
| | 1 | 2 | 3 | 4 | 5 | 6 | 7 | 8 | 9 | 10 | | |
| 1 | 21.87 | 2.73 | 21.9 | 1.67 | 8.09 | 10.28 | 39.24 | - | 6.52 | 2.73 | 8.09 | 12.78 ± 12.54 |
| 2 | 15.03 | 16.64 | 18.81 | 0.12 | 0.64 | 10.35 | 31.36 | 1.68 | 3.76 | 14.49 | 12.42 | 11.29 ± 10.00 |
| 3 | 32.41 | 7.26 | 23.41 | 15.39 | 14.88 | 1.07 | 44.33 | - | 22.5 | - | 18.94 | 20.16 ± 13.79 |
| 4 | 3.62 | - | 14.55 | 14.61 | 21.1 | 12.77 | 35.87 | - | 34.54 | 3.36 | 14.58 | 17.55 ± 12.38 |

the dependency of the detection result from the position of the radar and to determine how flexible our system is. For a systematic evaluation of the radar sensor signals, a series of measurements is conducted on 10 test persons. For each test person, measurements were performed from four different positions. The mean of the heart and respiration rate is determined and the relative error compared to the mean of the reference data is calculated.

In Table II, the results of the relative error for the respiration rate are summarized. Positions 1 (frontal, distance 1m) and 4 (frontal, distance of 2m) show promising results with a median of the relative error of 6.89 % and 5.52 %, respectively. This result is reasonable, as the thorax predominantly expands in the frontal plane (ventral) during breathing. Nevertheless, measurements of the respiration rate from position 3 (left lateral) are possible as well with a median relative error of 9.75 %.

The results concerning the measured heart rates are summarized in Table III. In general, the relative error of the heart rate is larger compared to the respiratory rate. Especially for the left side position and front position with 2 m distance, the median relative error is larger with 18.94 % and 14.58 %, respectively. In contrast to the respiration detection these two positions are less suitable for detecting the heart rate. The best result is achieved with the frontal position at 1 m distance with a median relative error of 8.09 %.

## IV. CONCLUSION

In this paper, the performance of an ultra-wideband FMCW-radar for vital sign detection is compared with a standard monitoring system. The respiration signal detected with the radar sensor is significantly correlated with the $CO_2$ reference measurement. Minimum relative errors can be achieved by placing the radar sensor in front of the thorax. Additionally the possibility of detecting the respiration rate from the left side position is shown. Moreover, the potential to detect the heart rate with the 80 GHz FMCW-radar is investigated. First results show promise, that even the heart rate can be measured contactless through clothing by high resolution FMCW-radar, although it is very challenging due to small skin surface movement caused by the cardiac activity. These results indicate, that robust contactless heart rate monitoring is feasible by FMCW-radar. Subsequent clinical studies should be carried out to examine potential clinical impact.

## REFERENCES


[1] C.I. Franks, B.H. Brown, D.M. Johnston, Contactless respiration monitoring of infants, Medical and Biological Engineering, vol. 14, pp. 306 - 312, June 1976.

[2] C. Li, V. Lubecke, O. Boric-Lubecke, J. Lin, A review on recent advances in Doppler radar sensors for noncontact healthcare monitoring, IEEE Trans. Microwave Theory and Techniques, vol. 61, pp. 2046 - 2060, May 2013.

[3] A. Droitcour, V. Lubecke, J. Lin, O. Boric-Lubecke, A microwave radio for Doppler radar sensing of vital signs, Microwave Symposium Digest, IEEE MTT-S International, vol. 1, pp. 175 - 178, May 2001.

[4] J. Muehlsteff, J. Thijs, R. Pinter, The use of a two channel Doppler radar sensor for the characterization of heart motion phases, IEEE Int. Conf. Engineering in Medicine and Biology Society, pp. 547 - 550, August 2006.

[5] D. Obeid, S. Sadek, G. Zaharia, G. Zein, Doppler radar for heartbeat rate and heart rate variability extraction, E-Health and Bioengineering Conference, pp. 1 - 4, November 2011.

[6] E.M. Staderini, UWB radars in medicine, IEEE Aerospace and Electronic Systems Magazine, vol. 17, pp. 13 - 18, January 2002.

[7] I. Immorev, Practical application of ultra-wideband radars, IEEE Int. Conf. Ultrawideband and Ultrashort Impulse Signals, pp. 44 - 49, September 2006.

[8] M. Singh, G. Ramachandran, Reconstruction of sequential cardiac in-plane displacement patterns on the chest wall by laser speckle interferometry, IEEE Trans Biomedical Engineering, vol. 38, pp. 483 - 489, May 1991.

[9] J.C. Lin, Microwave sensing of physiological movement and volume change: A review, Bioelectromagnetics, vol. 13, pp. 557 - 65, January 1992.

[10] N. Pohl, T. Jaeschke, K. Aufinger, An ultra-wideband 80 GHz FMCW radar system using SiGe bipolar bransceiver chip stabilized by a fractional-N PLL synthesizer, IEEE Trans. Microwave Theory and Techniques, vol. 60, pp. 757 - 765, March 2012.

[11] N. Pohl, T. Jaeschke, S. Scherr, S. Ayhan, M. Pauli, T. Zwick, T. Musch, Radar measurements with micrometer accuracy and nanometer stability using an ultra-wideband 80 GHz radar system, IEEE Conf. Wireless Sensors and Sensor Networks, pp. 31 - 33, January 2013.

[12] Council of the European Union (1999/519/EC), Council Recommendation on the limitation of exposure of the general public to electromagnetic fields, July 1999.

[13] M. Köny, J. Benzko, M. Czaplik, M. Walter, K. Radermacher, R. Rossaint, S. Leonhardt, Getting anasthesia online: The smartOR network, International Journal On Advances in Internet Technology, vol. 5, pp. 114-125, December 2012.